



# Methane oxidation over a honeycomb Pd-only three-way catalyst under static and periodic operation



Daive Ferri<sup>a,\*</sup>, Martin Elsener<sup>a</sup>, Oliver Kröcher<sup>a,b</sup>

<sup>a</sup> Paul Scherrer Institute, CH-5232 Villigen PSI, Switzerland

<sup>b</sup> École polytechnique fédérale de Lausanne (EPFL), Institute for Chemical Sciences and Engineering, CH-1015 Lausanne, Switzerland

## ARTICLE INFO

### Article history:

Received 17 June 2017

Received in revised form 20 July 2017

Accepted 24 July 2017

Available online 25 July 2017

### Keywords:

Natural gas

Three-way catalyst

Palladium

Rich/lean operation

Lambda

Operando spectroscopy

## ABSTRACT

Natural gas is receiving increasing awareness as fuel for passenger vehicles due to its very low specific CO<sub>2</sub> emissions. However, control of CH<sub>4</sub> emissions from natural gas combustion in stoichiometric engines requires a specific three-way catalyst (TWC). The understanding of the TWC chemistry of CH<sub>4</sub> under the periodic rich/lean reaction conditions is a key issue for targeted catalyst development. A commercial Pd-only TWC was tested under various reaction conditions to characterize the chemical processes and the mode of operation leading to efficient operation. It was demonstrated that periodic rich/lean operation obtained by variation of the mean O<sub>2</sub> concentration fed to the catalyst with various amplitudes is highly beneficial for CH<sub>4</sub> oxidation. Especially asymmetric oscillations into rich of stoichiometry produced higher CH<sub>4</sub> conversion. Compared to operation with gasoline fuel using propene as the model hydrocarbon, substantial differences were observed in static experiments that reflect the different chemistry at work with the two hydrocarbons. In particular, the stoichiometric point ( $\lambda = 1$ ) did not coincide with maximum CH<sub>4</sub> oxidation, which was obtained rather under rich conditions. The shift of the optimum stoichiometric point was associated with the necessity to consume CO and O<sub>2</sub> before CH<sub>4</sub> can react. Spectroscopic characterization during reaction aimed at rationalizing the role of NO in isothermic experiments when varying stepwise the oxygen concentration from net oxidizing to net reducing reaction conditions. The overall results should provide recommendations for the design of TWC for natural gas operation and for control strategies to improve CH<sub>4</sub> emission levels.

© 2017 Elsevier B.V. All rights reserved.

## 1. Introduction

Natural gas plays a central role for the reduction of CO<sub>2</sub> road emissions, especially because of the growing importance of addition of bio-gas and synthetic natural gas to the existing distribution network. Vehicles fueled with natural gas and bio-gas are powered by either stoichiometric or lean burn engines depending on the size and purpose of the vehicle. Emissions of methane (CH<sub>4</sub>), the major component of these fuels, remain a concern because of its global warming potential and are thus controlled efficiently by exploiting catalytic converters [1]. Three-way catalysts (TWC) represent the current technology in the case of the exhaust of natural gas passenger vehicles operating with stoichiometric engines [2,3]. The catalyst composition is adapted from the gasoline TWC counterpart by additional platinum group metals (PGM), mostly palladium (Pd), in order to improve the efficiency of CH<sub>4</sub> oxidation, which is

more difficult to activate than longer chain hydrocarbons representative of gasoline exhaust (propane, propene) [4]. A stoichiometric air-to-fuel ratio ( $\lambda = 1$ ) is required for the TWC operation in order to remove simultaneously the three pollutants, CO, NO and hydrocarbons [5]. This type of operation is characterized by the point at which CO oxidation activity increases to full conversion and the NO reduction activity decreases simultaneously while moving towards lean conditions [6], the CO-NO crossover point [7]. Around this point, the conversion of the three pollutants is most efficient. It is known [7–10] that in the case of TWC for natural gas fuel this point does not correspond to stoichiometry ( $\lambda = 1$ ) but is shifted into slightly rich of stoichiometry, essentially because of the low reactivity of CH<sub>4</sub>. This practical observation reflects also the different chemistry of abatement of the exhaust pollutants between gasoline and natural gas. Despite the extensive knowledge on the chemistry of CH<sub>4</sub> oxidation on PGM based catalysts under lean conditions [11–17] that in the automotive sector pertains to lean burn engines of large vehicles, e.g. buses and trucks, a systematic investigation of the complex chemistry involved in CH<sub>4</sub> oxidation on TWC is rare. On the one side, this knowledge is crucial for the design of cat-

\* Corresponding author.

E-mail address: [daive.ferri@psi.ch](mailto:daive.ferri@psi.ch) (D. Ferri).

alysts specialized on the abatement of emissions from natural gas fueled engines in contrast to catalysts for gasoline operation. On the other side, the knowledge should also be used to develop catalyst control strategies tailored for operation with this fuel. While little information is available on the behavior of simplified catalyst formulations, which are desirable in order to rationalize the involved chemistry, the majority of the studies in the open literature focused on the characterization of complex or even commercial TWC compositions. A rigorous derivation of the mutual effects of chemical and material components is difficult based on these premises. Subramanian et al. [10] were the first to subject a Pd/Al<sub>2</sub>O<sub>3</sub> catalyst to various reaction environments with the aim to derive the essential chemistry of CH<sub>4</sub> oxidation on a TWC. Besides reporting higher CH<sub>4</sub> conversion under reducing conditions than under oxidizing conditions, critical observations revealed a substantial inhibition of CH<sub>4</sub> oxidation in the presence of CO under net oxidizing conditions. Moreover, CH<sub>4</sub> oxidation by NO was emphasized as a route for CH<sub>4</sub> removal under net reducing conditions, while steam reforming was considered negligible, in marked contrast to observations by others on commercial catalysts of complex composition [18,19] and on Pt-Rh/CeO<sub>2</sub>-Al<sub>2</sub>O<sub>3</sub> [20]. The presence of the oxygen storage component (Ce) and of rhodium may contribute to explain the beneficial role of steam on CH<sub>4</sub> conversion. Additionally, NO reduction by hydrogen (NO + H<sub>2</sub>) and by CH<sub>4</sub> (CH<sub>4</sub> + NO) were identified at different temperature regimes [18,20]. Hence, it is important to underline that the typical reaction responsible for NO reduction on gasoline TWC, i.e. CO + NO, does not contribute appreciably when CH<sub>4</sub> is the hydrocarbon. These data were obtained predominantly under static reaction conditions exploiting temperature programmed ramps in either rich or lean feeds and lambda sweeps, where the air-to-fuel equivalence ratio is varied stepwise at various temperatures. Bounechada et al. [19] analyzed this chemistry on a commercial Pd-Rh-Al-Ce catalyst under periodic rich/lean reaction conditions that better mimic the operating conditions of the TWC. It was demonstrated that short rich pulses can sustain CH<sub>4</sub> oxidation at higher conversion levels than static experiments and that small amplitude oscillations of O<sub>2</sub> concentration around stoichiometry were more beneficial than large amplitude oscillations. Hence, these experimental conditions are favorable to CH<sub>4</sub> oxidation compared to either rich or lean conditions.

Here, we demonstrate the beneficial effects of the periodic operation of a Pd-only TWC for the abatement of CH<sub>4</sub> compared to steady state operation. We also attempt to show the influence of CO, NO and oxidation state of Pd on the CH<sub>4</sub> oxidation activity on a catalyst of reduced complexity and functionality (only one PGM).

## 2. Experimental

The catalyst used in this study was a full-size honeycomb Pd-only three-way catalyst (56.6 g/ft<sup>2</sup> Pd; 600 cpsi) kindly provided by Umicore containing Al, Ce, Zr and promoters in unknown ratios. Prior to use, the full-size monolith was degreened in static air at 600 °C for 10 h.

### 2.1. Catalytic measurements

Monolith pieces of 2.3 × 1.8 × 1.2 cm<sup>3</sup> were cut from the full-size monolith and used for the catalytic measurements. The reactor was adapted from the one described previously for the selective catalytic reduction of NO [21]. Gases were dosed by electronic mass flow controllers (Brooks), while water was provided through a water evaporator. The monolithic sample was wrapped with ceramic tape, inserted in a homemade steel support and placed in a quartz tube in which the inlet zone upstream the sample was filled with ceramic beads to preheat and mix the gas feed. The reactor

was heated using three independent heating tapes while the temperature was read upstream and downstream the sample by two thermocouples inserted in the middle of the quartz tube. All gas lines were of stainless steel and were heated to 170 °C to avoid water condensation. The outlet of the reactor was interfaced to a FTIR spectrometer (Thermo Nicolet, 2 m gas cell heated to 180 °C) to measure online the concentrations of CH<sub>4</sub>, CO, NO, CO<sub>2</sub>, H<sub>2</sub>O, N<sub>2</sub>O, NH<sub>3</sub> and a mass spectrometer (Pfeiffer Omnistar) equipped with a stainless steel capillary (d<sub>i</sub> = 0.12 mm) heated to 180 °C to monitor the concentrations of O<sub>2</sub> and H<sub>2</sub>.

If not otherwise specified, the feed to the catalyst consisted of 1500 ppm CH<sub>4</sub>, 1600 ppm NO, 7000 ppm CO and 5 vol% water (bal. N<sub>2</sub>) representative of the exhaust of a natural gas vehicle and the catalyst load was GHSV = 75000 h<sup>-1</sup>. According to the definition of λ [22], 5700 ppm O<sub>2</sub> were added to the continuous feed for stoichiometric dosage of oxygen, corresponding to nominal λ = 1. For the periodic oscillations, the mass flowmeters controlling the flowrates of oxygen and nitrogen were programmed to oscillate between given values as indicated. This together with the characteristic time of analysis of the residual gas products and the residence time of the reactor limits the pulse frequency that we can achieve to 5 s.

Conversion values of CH<sub>4</sub>, CO and NO are provided as X<sub>i</sub>(%) = 100 × (C<sub>i0</sub> - C<sub>i</sub>)/C<sub>i0</sub>, where C<sub>i0</sub> and C<sub>i</sub> are the initial concentration of the i<sup>th</sup> component in the feed (upstream of the catalyst) and its concentration downstream of the catalyst, respectively.

### 2.2. Spectroscopic measurements

Diffuse reflectance UV-vis (DRUV) and infrared Fourier transform (DRIFT) spectroscopy measurements were performed using the same gas feeding system described above for the catalytic measurements. For these measurements, the catalytic reactor was by-passed and the feed gas was directed either to the UV-vis spectrometer (Cary 4000, Agilent) or the FTIR spectrometer (Vertex 70, Bruker). The sample was cut from the full-size monolith and crashed to fine powder before mounting in the diffuse reflectance reactor cell attached to a Praying Mantis mirror unit (Harrick) fitting both spectrometers.

DRUV and DRIFT spectra were collected at steady state at 350 °C while decreasing stepwise the O<sub>2</sub> partial pressure in the CH<sub>4</sub>-CO-H<sub>2</sub>O and CH<sub>4</sub>-NO-CO-H<sub>2</sub>O feeds from 7000 ppm to 0 ppm. DRUV spectra were obtained between 400 and 800 nm. DRIFT spectra were acquired at 4 cm<sup>-1</sup> resolution between 4000 and 1000 cm<sup>-1</sup> by co-adding 50 interferograms. The background spectrum was obtained at 350 °C prior to admittance of the reaction feed.

## 3. Results and discussion

### 3.1. Temperature programmed reaction

Periodic rich/lean reaction conditions are beneficial for the efficiency of a three-way catalyst (TWC) [23] also for aftertreatment of natural gas vehicles [19] and represent realistic operation conditions. The effect of oscillating reaction conditions was verified on the Pd-only honeycomb catalyst and compared to steady state reaction conditions. Methane (CH<sub>4</sub>) conversion in continuous stoichiometric feed representative of the exhaust gas of natural gas fueled engines proceeded as shown in Fig. 1. Light-off occurred at ca. 350 °C but CH<sub>4</sub> conversion was not complete even at 600 °C and the maximum value was ca. 30%. Despite the impossibility to control the catalyst composition, meaning that possibly other catalysts could provide better performance, the data reveals the difficulty to remove CH<sub>4</sub> from exhaust gases under steady state stoichiometric conditions (λ = 1) questioning the suitability of this type of mea-

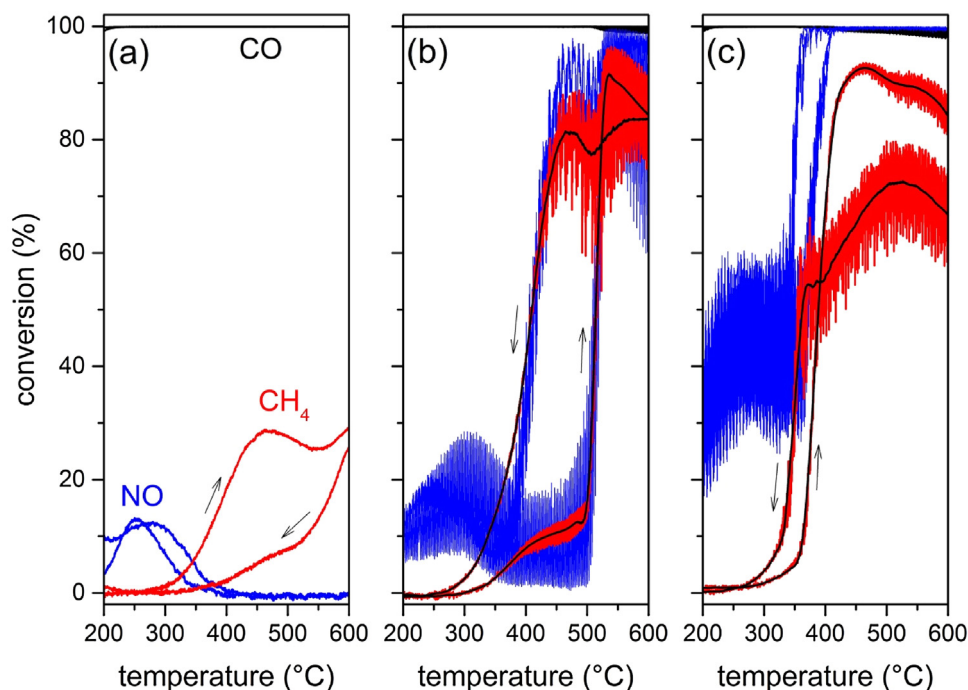


**Fig. 1.** CO (black), NO (blue) and CH<sub>4</sub> (red) conversions obtained from ascending and descending linear temperature ramps (a) in continuous stoichiometric feed, (b) in oscillating feed with symmetric O<sub>2</sub> pulses of 1000 ppm around stoichiometry (corresponding to mean 5700 ppm O<sub>2</sub>) and (c) in oscillating feed with symmetric O<sub>2</sub> pulses of 1500 ppm around  $\lambda = 0.992$  (corresponding to mean 4200 ppm O<sub>2</sub>). The dark lines within the conversion profiles of CH<sub>4</sub> represent the mean conversion. Arrows indicate direction of ramp segment. (For interpretation of the references to colour in this figure legend, the reader is referred to the web version of this article.)

measurements for the evaluation of the TWC on a honeycomb catalyst. Full CH<sub>4</sub> conversion was observed at ca. 500 °C under comparable feed composition on a model Pd-Al<sub>2</sub>O<sub>3</sub>-CeO<sub>2</sub>-ZrO<sub>2</sub> TWC in powder form [24]. The limited CH<sub>4</sub> oxidation activity achieved with the present catalyst needs to be attributed to the vastly different conditions inherent to experimentation with honeycomb monolith and powder catalysts, e.g. the space velocity or catalyst load. A significant negative hysteresis was observed in the cooling segment, CH<sub>4</sub> conversion being only ca. 5% at 450 °C. This picture changed significantly when the concentration of oxygen in the feed was varied symmetrically around stoichiometry by  $\pm 1000$  ppm (i.e. between 4700 and 6700 ppm, 5700 ppm O<sub>2</sub> being the nominal stoichiometric point) with a pulse duration of 15 s during heating and 5 s during cooling between 200 to 650 °C. This measurement simulated the periodic conditions that may be encountered during operation of the TWC under realistic conditions. The average conversion remained below 15% below 500 °C while it increased steeply above 500 °C reaching ca. 90% at 550 °C, standing in marked contrast to the result obtained with the continuous stoichiometric feed. The temperature of 50% conversion of CH<sub>4</sub> ( $T_{50}$ ) was ca. 510 °C in the heating segment and ca. 410 °C in the cooling segment indicative of a positive hysteresis, contrary to the temperature programmed reaction in continuous feed. The periodic variation of the O<sub>2</sub> concentration was responsible for the pronounced periodic variation of the CH<sub>4</sub> conversion when the temperature was raised.

NO conversion was negligible above 350 °C in continuous feed while it followed essentially the behavior of CH<sub>4</sub> conversion during the periodic operation around stoichiometry in agreement with previous observations [20]. In particular, when CH<sub>4</sub> conversion started increasing at 500 °C, NO conversion increased simultaneously reaching an average value higher than 70% above 550 °C. In the cooling segment of the oscillating temperature programmed ramp, the same hysteresis observed for CH<sub>4</sub> recurred for NO, and NO conversion sharply dropped to below 30% at 350 °C. Since short excursion into net reducing conditions was beneficial to CH<sub>4</sub> oxi-

dation, the  $\lambda$  cycling experiment was repeated with a maximum  $\lambda$  value corresponding to stoichiometry (i.e. between 2700 and 5700 ppm O<sub>2</sub>) and the average O<sub>2</sub> concentration in the feed gas under net reducing conditions. Hence, when the O<sub>2</sub> concentration was varied by  $\pm 1500$  ppm symmetrically around  $\lambda = 0.992$  (corresponding to a mean value of 4200 ppm O<sub>2</sub>; every 5 s),  $T_{50}$  further decreased significantly (370 °C and 350 °C in the heating and cooling segments, respectively), which was mirrored by the improved low temperature abatement of NO. The average NO conversion was ca. 40% until 350 °C and increased to full conversion at 400 °C. N<sub>2</sub>O was produced below 350 °C (max. 200 ppm) while NH<sub>3</sub> was detected above 400 °C with a maximum of 430 ppm at ca. 500 °C suggesting a possible change of NO reduction pathway (not shown) [18]. A positive hysteresis in CH<sub>4</sub> oxidation was observed also in the cooling segment but was accompanied by lower mean conversion between 600 and 350 °C than in the heating segment. CO conversion was always complete in the temperature range 200–600 °C except for a slight decrease in this latter experiment likely as a result of the large excursion into reducing conditions.

The data of Fig. 1 demonstrates clearly that CH<sub>4</sub> oxidation can be significantly improved upon variation of the feed concentration of oxygen repeatedly. This produces lower light-off temperatures and allows the attainment of higher CH<sub>4</sub> conversion at lower temperature. NO<sub>x</sub> abatement proceeds parallel to CH<sub>4</sub> conversion confirming earlier observations indicating that the kinetics of NO reduction is controlled by that of the CH<sub>4</sub>-O<sub>2</sub> reaction [8]. Moreover, oxygen pulsing under net rich conditions provided lower light-off temperatures of both pollutants.

### 3.2. Isothermic CH<sub>4</sub> oxidation

Based on the previous results, we studied CH<sub>4</sub> oxidation by varying stepwise the concentration of oxygen in the feed, because this parameter affected significantly the activity in a wide temperature regime. These measurements are essentially coinciding with

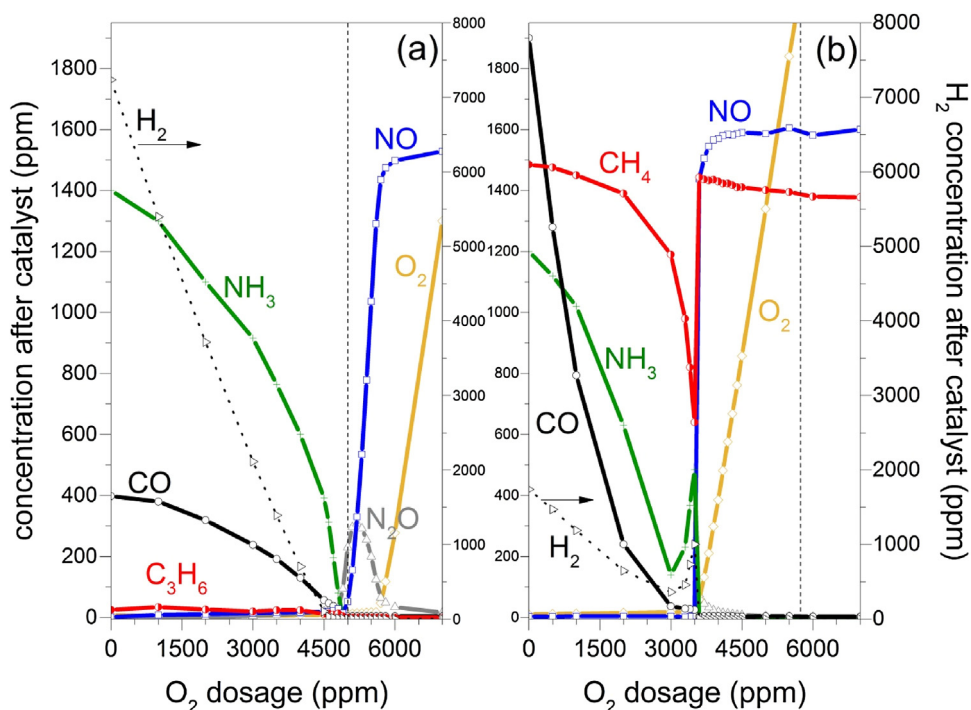


**Fig. 2.** Concentrations of CO, NO, C<sub>3</sub>H<sub>6</sub>, CH<sub>4</sub>, O<sub>2</sub>, H<sub>2</sub>, NH<sub>3</sub> and N<sub>2</sub>O after catalyst at 425 °C in continuous feed of (a) 7000 ppm CO, 1600 ppm NO, 500 ppm C<sub>3</sub>H<sub>6</sub> (equivalent to 1500 ppm C<sub>1</sub>), 5 vol% H<sub>2</sub>O and (b) 7000 ppm CO, 1600 ppm NO, 1500 ppm CH<sub>4</sub>, 5 vol% H<sub>2</sub>O while decreasing the O<sub>2</sub> concentration from 7000 to 0 ppm. The vertical dash lines mark the position for stoichiometry (see text for details). (For interpretation of the references to colour in this figure legend, the reader is referred to the web version of this article.)

measurements where the air-to-fuel ratio (or  $\lambda$ ) is varied and the conversion of CH<sub>4</sub> and of the other pollutants is followed at selected temperatures. Therefore, besides CH<sub>4</sub>, NO<sub>x</sub> and CO were also added to the feed to the catalyst in order to follow possible effects of the additional pollutants on CH<sub>4</sub> oxidation performance of the catalyst. Additionally, we carried out similar experiments where the mean O<sub>2</sub> concentration was decreased stepwise rather than the absolute O<sub>2</sub> concentration and the amplitude of the O<sub>2</sub> concentration was varied around selected values. The amplitude was kept constant while increasing the mean O<sub>2</sub> concentration value, and the measurements were repeated at various O<sub>2</sub> concentration amplitudes.

First, we compare the results obtained with CH<sub>4</sub> with those obtained using propene (C<sub>3</sub>H<sub>6</sub>) as the representative hydrocarbon residue of engine fueled by gasoline. The concentration of propene is typically lower than that of CH<sub>4</sub>, while the other pollutants (CO and NO<sub>x</sub>) can be considered within the same order of magnitude. The concentration of propene was selected on the base of C<sub>1</sub> equivalents.

Fig. 2 demonstrates the results obtained at 425 °C while decreasing the O<sub>2</sub> concentration in the feed in order to achieve the stepwise variation of  $\lambda$ . Fig. 2a shows the data for propene. The concentration of propene was negligible along the whole range of O<sub>2</sub> concentrations that we explored in line with the ease of activation of this hydrocarbon [7]. The variation of NO<sub>x</sub> and CO concentrations in Fig. 2a is consistent with the typical description of the operation of a TWC [25]. The CO-NO crossover point lies clearly at stoichiometry (4950 ppm O<sub>2</sub> in the case of propene). As expected, NO conversion sharply decreased with increasing O<sub>2</sub> concentration above the value corresponding to stoichiometry, while CO concentration increased under increasingly rich conditions. Fig. 2a also shows that NO conversion started decreasing when the O<sub>2</sub> concentration downstream the catalyst was nil. Non negligible amounts of ammonia (NH<sub>3</sub>, maximum 1400 ppm) were detected under rich conditions simultaneous to the emission of hydrogen (>7000 ppm). Hence, steam reforming of propene took place in net rich conditions

and NO reduction (likely to NH<sub>3</sub>) occurred through the produced hydrogen. Nitrous oxide was also detected for higher O<sub>2</sub> concentrations than 4700 ppm indicating the non-selective reduction of NO slightly above the stoichiometric value.

Fig. 2b clearly demonstrates that removal of CH<sub>4</sub> from the exhaust under the same experimental conditions was substantially different. CH<sub>4</sub> conversion at 425 °C occurred between 500 and 3600 ppm O<sub>2</sub> with a maximum conversion level of ca. 60% at 3500 ppm O<sub>2</sub>, which decreased very sharply towards higher O<sub>2</sub> concentration. Then, it increased slowly up to less than 10% at 6000 ppm O<sub>2</sub>. Contrary to propene, the window of CH<sub>4</sub> conversion was very narrow and conversion was low, in agreement with the difficulty to activate CH<sub>4</sub> compared to propene and propane [7].

The major difference between Fig. 2a and b is that the CO-NO crossover point in the case of CH<sub>4</sub> did not correspond to stoichiometry (in this case, 5700 ppm O<sub>2</sub>) contrary to the case of propene but occurred at 3500 ppm O<sub>2</sub>. We define the stoichiometry value necessary to remove CH<sub>4</sub> most efficiently as:

$$R_{O_2/nM} = C_{O_2} \times 2 / C_{CO} \quad (1)$$

where  $C_{O_2}$  and  $C_{CO}$  are the oxygen and carbon monoxide concentrations, respectively.  $R_{O_2/nM}$  corresponds to the stoichiometric factor often reported in the literature [26], with the exception that the concentrations of NO and of the hydrocarbon do not appear in Eq. (1). Hence,  $R_{O_2/nM}$  considers CH<sub>4</sub> as an inert gas, while NO is not considered because it follows tightly the behavior of CH<sub>4</sub> (Fig. 2b). Above this point (lean conditions) CH<sub>4</sub> concentration increased instantaneously while below this point (rich conditions) the increase of CH<sub>4</sub> concentration was smoother. It is clear from Fig. 2b that CH<sub>4</sub> was removed efficiently from the gas feed in correspondence of the point where CO is completely oxidized in agreement with Eq. (1). CO concentration was ca. 40 ppm at 3000 ppm O<sub>2</sub> and decreased below 5 ppm at 3600 ppm O<sub>2</sub>. The remaining oxygen provided to the catalyst can then be used to oxidize CH<sub>4</sub>. This behavior can be ascribed to the easier adsorption



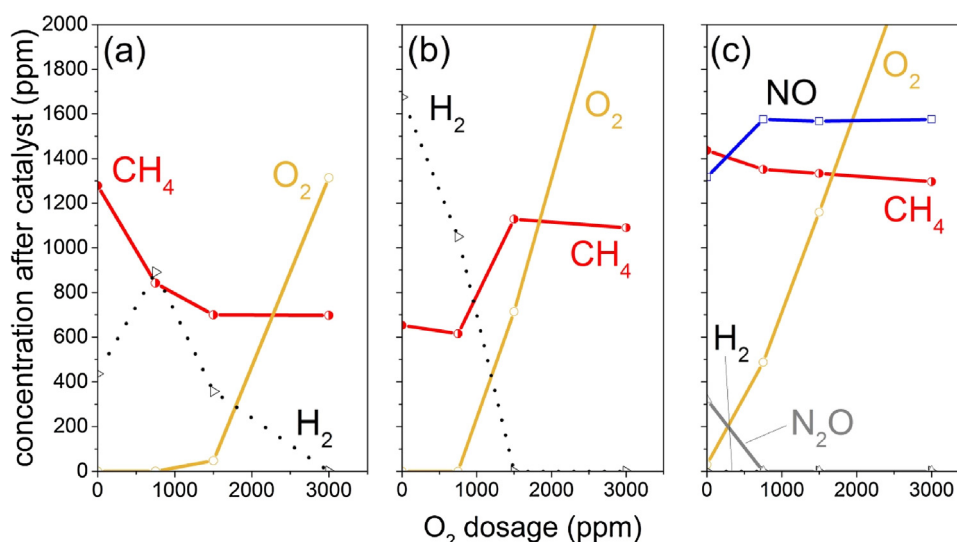


**Fig. 3.** Concentrations of  $\text{CH}_4$ ,  $\text{O}_2$ ,  $\text{H}_2$ ,  $\text{NO}$  and  $\text{N}_2\text{O}$  after catalyst at  $425^\circ\text{C}$  in continuous feed of (a) 1500 ppm  $\text{CH}_4$ , (b) 1500 ppm  $\text{CH}_4$ , 5 vol%  $\text{H}_2\text{O}$  and (c) 1500 ppm  $\text{CH}_4$ , 1600 ppm  $\text{NO}$ , 5 vol%  $\text{H}_2\text{O}$  while decreasing the  $\text{O}_2$  concentration from 3000 ppm to nil. The real  $\text{H}_2$  concentration in (b) is twice that displayed. (For interpretation of the references to colour in this figure legend, the reader is referred to the web version of this article.)

and reaction of  $\text{CO}$  that cause inhibition of  $\text{CH}_4$  oxidation [10] and confirms the impression that the two reactions occur on similar if not identical active sites [27].

Hydrogen was detected also in the case of  $\text{CH}_4$ . However, its concentration attained the highest value in correspondence of the maximum  $\text{CH}_4$  conversion suggesting that steam reforming indeed contributed significantly to  $\text{CH}_4$  oxidation under net rich conditions [18–20] also on the Pd-only TWC. Evolution of  $\text{NH}_3$  mirrored the formation of  $\text{H}_2$  confirming that reduction by  $\text{H}_2$  is a crucial  $\text{NO}$  abatement pathway [18]. It is significant to note that in contrast to propene, no  $\text{N}_2\text{O}$  formation was detected around the point of maximum hydrocarbon conversion. From a practical perspective, Fig. 2 clearly demonstrates that the chemistry of abatement of the major pollutants ( $\text{CO}$ ,  $\text{NO}$  and hydrocarbon) from stoichiometric engines fueled with gasoline and natural gas is very different. This implies that the TWC for natural gas operation needs to be developed independently.

Given the complex behavior of the catalyst in presence of all pollutants, we investigated the reciprocal effects of water and  $\text{NO}$  on the chemistry of  $\text{CH}_4$  oxidation in more detail by performing experiments where the  $\text{O}_2$  concentration was scanned stepwise between 3000 ppm and 0 ppm at constant feed concentration of 1500 ppm  $\text{CH}_4$ . This approach may appear redundant with other studies mentioned here, but it is justified by the fairly different catalyst composition and highlights again the need for systematic investigations on model catalysts of increasing complexity. We did not address specifically the influence of  $\text{CO}$  because of the clear inhibiting effect observed in Fig. 2b and because of the parallel reactions  $\text{CO}$  can experience (e.g. water gas shift, WGS). Initially, the feed consisted only of  $\text{CH}_4$  and  $\text{O}_2$ , hence demonstrating the effect of  $\text{O}_2$  concentration on  $\text{CH}_4$  oxidation. The experiment was repeated with 5 vol%  $\text{H}_2\text{O}$  added to the feed and finally once more with 1600 ppm  $\text{NO}$  added to the  $\text{CH}_4$ - $\text{O}_2$ - $\text{H}_2\text{O}$  feed (Fig. 3).  $\text{CH}_4$  conversion was 43% at  $425^\circ\text{C}$  when 3000 ppm  $\text{O}_2$  were dosed (Fig. 3a), in agreement with the fact that this point represents stoichiometric conditions. When  $\text{O}_2$  was dosed in sub-stoichiometric amounts, the production of  $\text{H}_2$  confirmed that  $\text{CH}_4$  oxidation by both oxygen and steam reforming is responsible for  $\text{CH}_4$  removal under such conditions. Since water was not dosed in this experiment,  $\text{CH}_4$  oxidation by oxygen is needed in order to produce the amount of water required for steam reforming. The increas-

ingly reducing conditions inhibit  $\text{CH}_4$  oxidation by oxygen and, as a consequence, also steam reforming vanished below 750 ppm  $\text{O}_2$  because less and less water was available as probed by the decreasing  $\text{H}_2$  concentration. The addition of water to the feed does not move the theoretical stoichiometric point (3000 ppm  $\text{O}_2$ ) but according to these considerations it should improve  $\text{CH}_4$  oxidation under rich conditions. Fig. 3b demonstrates that  $\text{CH}_4$  conversion was lower than in the absence of water until 1500 ppm  $\text{O}_2$  likely because of the well-known inhibiting effect of water associated with the formation of Pd-OH species [28]. Steam reforming became important only below 1500 ppm  $\text{O}_2$  and did not extinguish with decreasing  $\text{O}_2$  concentration in contrast to Fig. 3a because of the constant presence of water in the feed. In the presence of  $\text{NO}$  (Fig. 3c) the stoichiometric point moved to 2200 ppm  $\text{O}_2$ .  $\text{CH}_4$  conversion changed from 13% under net lean conditions (3000 ppm  $\text{O}_2$ ) to 5% in the absence of  $\text{O}_2$ .  $\text{NO}$  conversion was negligible, but increased to 19% when the  $\text{O}_2$  concentration was lowered to almost zero in agreement with the observations of Fig. 2b. In this case, the  $\text{NO}$  conversion was accompanied by  $\text{N}_2\text{O}$  formation while no  $\text{NH}_3$  was observed. The absence of  $\text{NH}_3$  and of significant  $\text{NO}$  conversion may question whether  $\text{CO}$  contributes to  $\text{NO}$  abatement indirectly through WGS and production of  $\text{H}_2$  when  $\text{CO}$  is present in the feed.  $\text{NO}$  could react with this  $\text{H}_2$  rather than through the  $\text{H}_2$  produced by  $\text{CH}_4$  steam reforming. However,  $\text{CH}_4$  conversion was so low in presence of  $\text{NO}$  that the inhibiting effect of  $\text{NO}$  could be responsible for poisoning the reaction pool.  $\text{NO}$  was found to compensate the inhibiting effect of water on Pd and PdPt catalysts under lean  $\text{CH}_4$  oxidation conditions [29], while in the absence of water we found an inhibiting effect of  $\text{NO}$  on a Pd/ $\text{Al}_2\text{O}_3$  under simulated stoichiometric conditions [27]. The model experiments of Fig. 3 show that  $\text{CH}_4$  oxidation activity decreased in the order of increasing feed complexity,  $\text{CH}_4 + \text{O}_2 > \text{CH}_4 + \text{O}_2 + \text{H}_2\text{O} > \text{CH}_4 + \text{O}_2 + \text{H}_2\text{O} + \text{NO}$ . Hence,  $\text{CH}_4$  oxidation by  $\text{O}_2$  is inhibited by water, as it is already known, but at low  $\text{O}_2$  concentrations steam reforming occurs while  $\text{CH}_4$  oxidation by both  $\text{O}_2$  and water is inhibited by  $\text{NO}$ .

Returning to the stepwise scan of  $\text{O}_2$  concentration in the full exhaust mixture, the behavior of  $\text{CH}_4$  at  $350^\circ\text{C}$  was qualitatively similar to that observed at  $425^\circ\text{C}$  except for the obvious lower levels of conversion (Fig. 4). However, the  $\text{CO}$ - $\text{NO}$  crossover point was shifted notably further to lower  $\text{O}_2$  concentration (2700 ppm,

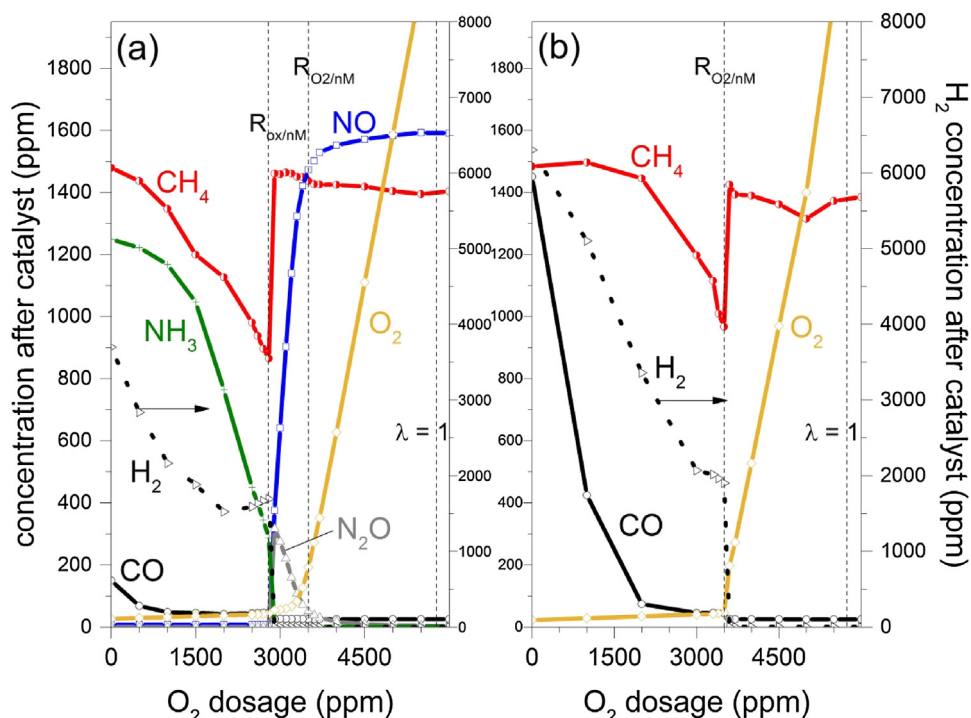


**Fig. 4.** Concentrations of CO, NO, CH<sub>4</sub>, H<sub>2</sub>, NH<sub>3</sub>, N<sub>2</sub>O and O<sub>2</sub> after catalyst at 350 °C in continuous feed of (a) 7000 ppm CO, 1500 ppm CH<sub>4</sub>, 1600 ppm NO, 5 vol% H<sub>2</sub>O and (b) 7000 ppm CO, 1500 ppm CH<sub>4</sub>, 5 vol% H<sub>2</sub>O while decreasing the O<sub>2</sub> concentration from 6000 ppm to nil. The vertical dash lines mark the position of  $R_{O_2/nM} = 1$ ,  $R_{ox/nM} = 1$  and  $\lambda = 1$  (see text for details). (For interpretation of the references to colour in this figure legend, the reader is referred to the web version of this article.)

Fig. 4a) to a new point that we define as the stoichiometric factor  $R_{ox/nM}$ .

$$R_{ox/nM} = (C_{O_2} \times 2 + C_{NO})/C_{CO} \quad (2)$$

now taking into account all oxidants, including  $C_{NO}$ , the NO concentration [26]. At this temperature N<sub>2</sub>O was produced (maximum 300 ppm) between 2700 and 3500 ppm O<sub>2</sub>. The further shift of the CO-NO crossover point towards richer reaction conditions prompted us to repeat the same measurement in absence of NO and by decreasing stepwise the O<sub>2</sub> concentration from 6000 ppm to 0 ppm to investigate the role of NO under these conditions. Fig. 4b shows that the concentration of CH<sub>4</sub> followed a similar behavior to that observed at 425 °C and exhibited a minimum value at 3500 ppm O<sub>2</sub> (ca. 33% conversion) with an abrupt increase for O<sub>2</sub> concentration above 3500 ppm and a smooth change below this value. The minimum in CH<sub>4</sub> concentration coincided again with the full conversion of O<sub>2</sub> and CO. The value of O<sub>2</sub> concentration at which CH<sub>4</sub> was efficiently converted and corresponding to the CO-NO crossover point defined in Eq. (1) ( $R_{O_2/nM}$ ) was identical to the value observed in presence of NO at 425 °C. Hence, at lower temperature, NO appears responsible for the shift of the window of efficient removal of CH<sub>4</sub> to lower O<sub>2</sub> concentrations that forced us to include it in the  $R_{ox/nM}$  stoichiometric factor. At low temperature the total concentration of the oxidizing agents becomes the limiting factor for CH<sub>4</sub> abatement. It should be noted that despite the shift of the stoichiometric factor, indicating that CH<sub>4</sub> removal is substantially more difficult, CH<sub>4</sub> conversion improved (ca. 47%) and broadened significantly into net rich conditions in presence of NO compared to the situation in absence of NO (ca. 33%) revealing a possible promoting effect of NO at low temperature. Upon careful inspection of the H<sub>2</sub> and NH<sub>3</sub> concentration values of Fig. 4a and b we speculate that CH<sub>4</sub> oxidation activity under reducing conditions in presence of NO is promoted by the removal of adsorbed hydrogen by NO from the catalyst. Nevertheless, the overall catalytic behavior described in Figs. 2–4 suggests that CO, NO and the

majority of oxygen need to be removed from the exhaust before CH<sub>4</sub> can react, thus reinforcing the opinion that CH<sub>4</sub> acts as an inert gas over a wide range of reaction conditions and that active sites for CH<sub>4</sub> oxidation need to be freed from competing reactions involving CO and NO.

### 3.3. Isothermic oscillating CH<sub>4</sub> oxidation

Based on the behavior observed in Fig. 1, similar measurements to those shown above (Fig. 2b) were repeated under periodic operation conditions. Hence, at fixed CO, NO and CH<sub>4</sub> concentrations, the mean O<sub>2</sub> concentration was decreased stepwise. The average O<sub>2</sub> concentration was the mean value obtained from pulses of increasing amplitudes. Experiments were repeated with O<sub>2</sub> dosages varying symmetrically between  $\pm 1000$ ,  $\pm 2000$  and  $\pm 3000$  ppm O<sub>2</sub> every 5 s. This pulse frequency is the one that we can presently attain with the described setup. Fig. 5(b–d) compare these experiments with that already shown in Fig. 2b for no periodic operation that is reported in simplified form in Fig. 5a (only CO, NO and CH<sub>4</sub> concentrations). Introduction of oscillations of  $\pm 1000$  ppm O<sub>2</sub> confirmed the beneficial effect of rich/lean periodic operation on CH<sub>4</sub> removal already observed in Fig. 1. CH<sub>4</sub> concentration increased abruptly at 4200 ppm O<sub>2</sub> when moving towards larger mean O<sub>2</sub> concentrations (Fig. 5b). It remained constant at 600 ppm (60% conversion) between 4200 and 3500 ppm O<sub>2</sub> before increasing smoothly below 3500 ppm O<sub>2</sub>. The abrupt change of CH<sub>4</sub> concentration at 4200 ppm O<sub>2</sub> coincided again with the CO-NO crossover point. Under these conditions, the hydrogen concentration (not shown) exhibited a peak maximum at  $R_{O_2/nM}$  (3500 ppm O<sub>2</sub>) and the NH<sub>3</sub> concentration decreased steadily with increasing the mean O<sub>2</sub> concentration from 1000 to 4500 ppm O<sub>2</sub>. Increasing the amplitude of the O<sub>2</sub> pulses to  $\pm 2000$  ppm (Fig. 5c) further increased CH<sub>4</sub> conversion with a maximum of ca. 77% at 5000 ppm O<sub>2</sub> and stretched the window of CH<sub>4</sub> conversion into the rich regime. Finally, CH<sub>4</sub> conversion was improved to a value

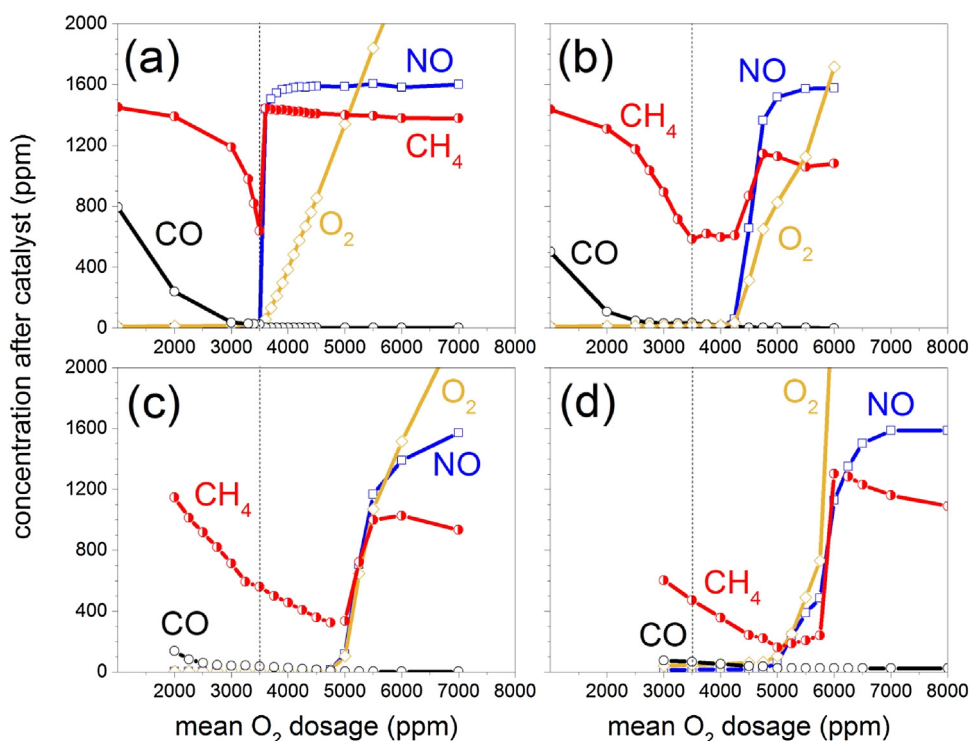


**Fig. 5.** Concentrations of CO, NO, CH<sub>4</sub> and O<sub>2</sub> after catalyst at 425 °C in (a) continuous feed of 7000 ppm CO, 1600 ppm NO, 1500 ppm CH<sub>4</sub>, 5 vol% H<sub>2</sub>O while decreasing the O<sub>2</sub> concentration from 7000 ppm to nil, and in oscillating feed with symmetric O<sub>2</sub> pulses of (b) 1000 ppm, (c) 2000 ppm and (d) 3000 ppm while decreasing the mean O<sub>2</sub> concentration. Pulse duration was 5 s. The vertical dash lines mark the position of  $R_{O_2/nM} = 1$  (see text for details). (For interpretation of the references to colour in this figure legend, the reader is referred to the web version of this article.)

of ca. 87% over a broad window (5700–4500 ppm O<sub>2</sub>) of operation when the amplitude was increased to  $\pm 3000$  ppm (Fig. 5d). The highest value of O<sub>2</sub> concentration of this window reached the point corresponding to the conventional stoichiometry value ( $\lambda = 1$ , 5700 ppm O<sub>2</sub>). These results are summarized in Fig. 6a for the sake of clarity for CH<sub>4</sub> and NO conversions as functions of pulse amplitude at constant pulse frequency (5 s). CH<sub>4</sub> conversion increased from ca. 58% in steady state operation to around 90% with pulses of  $\pm 3000$  ppm amplitude. The most notable change was that the window of operation of the Pd-only TWC broadened significantly as a function of pulse amplitude indicating that compared to the very narrow window observed under steady state conditions (Fig. 2b) [7] periodic operation could relax the optimal control conditions required to achieve efficient CH<sub>4</sub> abatement. N<sub>2</sub>O was detected with a maximum concentration of 117 ppm at  $\pm 3000$  ppm O<sub>2</sub> that moved following the shift of the CO–NO crossover point towards the stoichiometry value, while NH<sub>3</sub> production vanished from between 2000 ppm and 5250 ppm O<sub>2</sub> without following significantly the shift of the CO–NO crossover point (not shown in Fig. 5). Our results showing a relationship between oscillation amplitude and CH<sub>4</sub> conversion does not match totally with the results reported in the only work that to our knowledge dealt with rich/lean periodic operation of a TWC for natural gas operation [19]. The discrepancy can be solved tentatively by considering the vastly different experimental conditions between that work, oscillations around stoichiometry, and this work, oscillations around moving O<sub>2</sub> concentration, but deserves certainly further consideration.

Despite the fact we have devoted less attention to this issue, Fig. 6b demonstrates that the pulse frequency had far less influence on CH<sub>4</sub> abatement than the pulse amplitude in the case of  $\pm 1000$  ppm O<sub>2</sub> pulses in agreement with previous observations [30]. In fact, CH<sub>4</sub> conversion decreased significantly with increasing pulse frequency. Moreover, despite its broadening from steady state operation to periodic operation, the window of O<sub>2</sub> concentra-

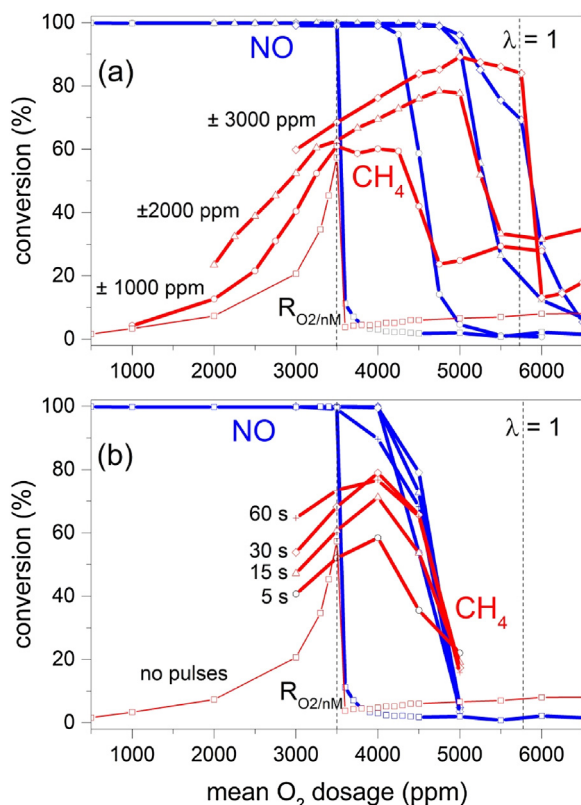
tion corresponding to optimal CH<sub>4</sub> abatement remained constant irrespective of pulse frequency. N<sub>2</sub>O (not shown) was detected between 4000 and 5000 ppm O<sub>2</sub> (maximum ca. 80 ppm at 5 s pulses) while NH<sub>3</sub> decreased steadily between 3000 and 5000 ppm O<sub>2</sub> from a maximum of 760 ppm in the pulse experiment with 60 s pulses.

Fig. 6 clearly demonstrates that the optimum CH<sub>4</sub> oxidation activity moved from the value of  $R_{O_2/nM}$  to that corresponding to stoichiometry with increasing pulse amplitude. It also shows once more the intimate correlation between CH<sub>4</sub> oxidation and NO reduction activities. Finally, it also suggests that high CH<sub>4</sub> abatement efficiency can be achieved by careful control of the rich/lean sequence.

### 3.4. Spectroscopy study

It is recognized that the oxidation state of Pd plays a key role in the chemistry of CH<sub>4</sub> oxidation on PGM based catalysts [11]. The stepwise scan of the O<sub>2</sub> concentration in static experiments and especially, the continuous rich/lean variation of the feed to the TWC in pulsed experiments can provoke a change of oxidation state that is responsible for the observed reactions under net reducing and net oxidizing conditions. Therefore, operando diffuse reflectance UV–vis (DRUV) and infrared (DRIFTS) spectroscopies were used to monitor the Pd oxidation state and the adsorbate speciation of the Pd-based catalyst, respectively while measuring the gaseous products by FTIR spectroscopy as described in the case of the catalytic reactor tests. Measurements were performed in a single cell directly attached to the gas setup used to feed the monolithic sample in order to ensure identical feed conditions to the reactor study. The O<sub>2</sub> concentration was decreased from 7000 to 0 ppm at 350 °C in order to work at a suitable temperature for infrared observation thus avoiding the influence of emission of infrared radiation from the sample at higher temperatures. Additionally, in order to evalu-





**Fig. 6.** (a) Amplitude and (b) frequency dependent  $\text{CH}_4$  and NO conversions corresponding to the data of Fig. 5. ( $\square$ ) Continuous feed of 7000 ppm CO, 1600 ppm NO, 1500 ppm  $\text{CH}_4$ , 5 vol%  $\text{H}_2\text{O}$  and stepwise decrease of  $\text{O}_2$  concentration; oscillating feed with symmetric  $\text{O}_2$  pulses of ( $\circ$ )  $\pm 1000$  ppm, ( $\triangle$ )  $\pm 2000$  ppm and ( $\diamond$ )  $\pm 3000$  ppm. The vertical dash lines mark the positions of  $R_{\text{O}_2/\text{nm}} = 1$  and  $\lambda = 1$  (see text for details). (For interpretation of the references to colour in this figure legend, the reader is referred to the web version of this article.)

ate the effect of NO on  $\text{CH}_4$  conversion from a chemical perspective, the  $\text{O}_2$  concentration sweeps were carried out in presence and in absence of NO in the feed. Hence, the experiments are equivalent to those shown in Fig. 4. Fig. 7 shows the DRUV spectra obtained under these experimental conditions. Despite the absence of any defined feature, a clear change occurred in the wide range of 450–800 nm while decreasing the  $\text{O}_2$  concentration in the feed irrespective of NO. This change was likely caused by variations of the plasmonic resonance of palladium particles [31,32] and we assign it to the oxidation state variation imposed by the PdO/Pd equilibrium under the specific environmental conditions applied during the experiment. We cannot exclude a significant contribution of  $\text{Ce}^{4+}/\text{Ce}^{3+}$  to the spectral changes, but the optical absorption edge of ceria and Ce-Zr solid solutions occurs typically below 450 nm [33]. The color change of the sample from brown to grey witnessed the spectroscopic observation of the change of oxidation state when moving from the high to the low  $\text{O}_2$  concentration regime (insets of Fig. 7), respectively. It is evident from the two series of spectra that the variation of this spectral region followed different kinetics depending on the presence of NO. In the absence of NO, an abrupt change occurred between 3250 and 3000 ppm  $\text{O}_2$  (Fig. 7a) while the change was smoother and occurred over a wider concentration regime (6000 and 1000 ppm  $\text{O}_2$ ) when NO was present in the feed (Fig. 7b).

If we turn our attention to  $\text{CH}_4$  conversion in these experiments, the result of this exercise was comparable to the catalytic data obtained at 350 °C (Fig. 4). The largest value of  $\text{CH}_4$  conversion in the absence of NO occurred at 3500 ppm  $\text{O}_2$  and extended towards lower  $\text{O}_2$  concentrations (ca. 2000 ppm  $\text{O}_2$ ; Fig. 8a). This value corresponds again to  $R_{\text{O}_2/\text{nm}} = 1$  as in the case of the catalytic activity

of the monolithic catalyst shown above and reflects the need of consuming  $\text{O}_2$  prior to the onset of conversion of  $\text{CH}_4$ . The course of  $\text{CH}_4$  conversion in Fig. 8a is further compared in Fig. 8b with the  $\text{O}_2$  concentration dependence of the point at 650 nm in the DRUV spectra taken as the descriptor of the change of Pd oxidation state. While decreasing the  $\text{O}_2$  concentration in the absence of NO,  $\text{CH}_4$  conversion changed from below 10% to ca. 35% at 3500 ppm  $\text{O}_2$ , when the intensity of the 650 nm point was low and thus the catalyst still largely oxidized as obvious from Fig. 8b. The abrupt change of oxidation state occurred immediately after the maximum of  $\text{CH}_4$  conversion. In the presence of NO, the highest value of  $\text{CH}_4$  conversion shifted from 3500 ppm  $\text{O}_2$  to 2750 ppm  $\text{O}_2$  (Fig. 8a) and coincided with the stoichiometric factor  $R_{\text{O}_2/\text{nm}}$  and with complete conversion of NO and  $\text{O}_2$ . The window of  $\text{O}_2$  concentration corresponding to optimum  $\text{CH}_4$  conversion remained broad and extended to ca. 500 ppm  $\text{O}_2$  but the increase of activity from below 5% to more than 40% coincided with a gradual change of the oxidation state monitored by DRUV spectroscopy (Fig. 7b) in marked contrast to the case without NO in the feed. Hence, the shift of the maximum  $\text{CH}_4$  conversion towards richer reaction conditions in the presence of NO coincided approximately with the point where the signal at 650 nm had almost reached the maximum of its ascent. It is clear that a close link exists between the catalytic parameters, e.g.  $\text{CH}_4$  conversion and the CO-NO crossover point (Fig. 8a), and the change of oxidation state delivered by DRUV (Fig. 8b).

The spectral region 2250–1250  $\text{cm}^{-1}$  of the DRIFT spectra collected during identical measurements is shown in Fig. 9a and Fig. 9b for the NO free and NO containing feeds, respectively. Some observations are common to the two experiments irrespective of NO. The spectra obtained at 7000 ppm  $\text{O}_2$  were dominated by signals between 1700 and 1300  $\text{cm}^{-1}$  that can be attributed to adsorbed carbonate species (1514, 1415 and 1340  $\text{cm}^{-1}$ , Table 1) [34]. Decreasing the  $\text{O}_2$  concentration caused a gradual increase of the carbonate coverage. The fraction of carbonates increased significantly and suddenly below 3250 ppm  $\text{O}_2$  in absence of NO and more gradually at 2000–1000 ppm  $\text{O}_2$  in presence of NO. This increase of surface coverage was accompanied by new signals at 1585 and 1376  $\text{cm}^{-1}$ , which together with those at 2907, 2838  $\text{cm}^{-1}$  (not shown, Table 1) are indicative of adsorption of formate species [35]. The origin of this species is likely to be found in the reducing conditions under which they formed and in the presence of Ce in the catalyst composition that promotes WGS and steam reforming reactions. Finally, a signal extending between 2050 and 1800  $\text{cm}^{-1}$  became increasingly visible, which was readily assigned to adsorbed CO on metallic Pd [36], together with the gas phase signature of unreacted CO (2200–2050  $\text{cm}^{-1}$ ). While no other specific feature characterized the spectra in absence of NO, the presence of NO in the feed at 7000 ppm  $\text{O}_2$  produced additional signals at 1545 and 1482  $\text{cm}^{-1}$  that we assign to adsorbed nitrates in various configurations [37–39]. While decreasing  $\text{O}_2$  concentration these species disappeared in the spectrum obtained at 2750 ppm  $\text{O}_2$ , which corresponds to the transition from the low to the high  $\text{CH}_4$  conversion regime in Fig. 8a. Hence,  $\text{CH}_4$  conversion becomes possible when NO has been consumed (Fig. 4) and the catalyst surface is free from NO-adsorbed species. This observation confirms our previous conclusion that NO inhibits  $\text{CH}_4$  oxidation through formation of adsorbed species [27]. Sadokhina et al. [29] assigned the inhibiting effect of NO in dry conditions to competition for active sites, while in the presence of water (similar to the conditions used in the present work) NO mitigated the water deactivation effect upon formation of  $\text{HNO}_2$  species.

All IR spectral changes were accompanied in both situations by strong baseline variations that were comparable to those observed for the signal at 650 nm in the DRUV spectra. Taking the point at 2500  $\text{cm}^{-1}$  as a descriptor of the baseline change, a point where no absorption is expected, the evolution of the baseline as a con-



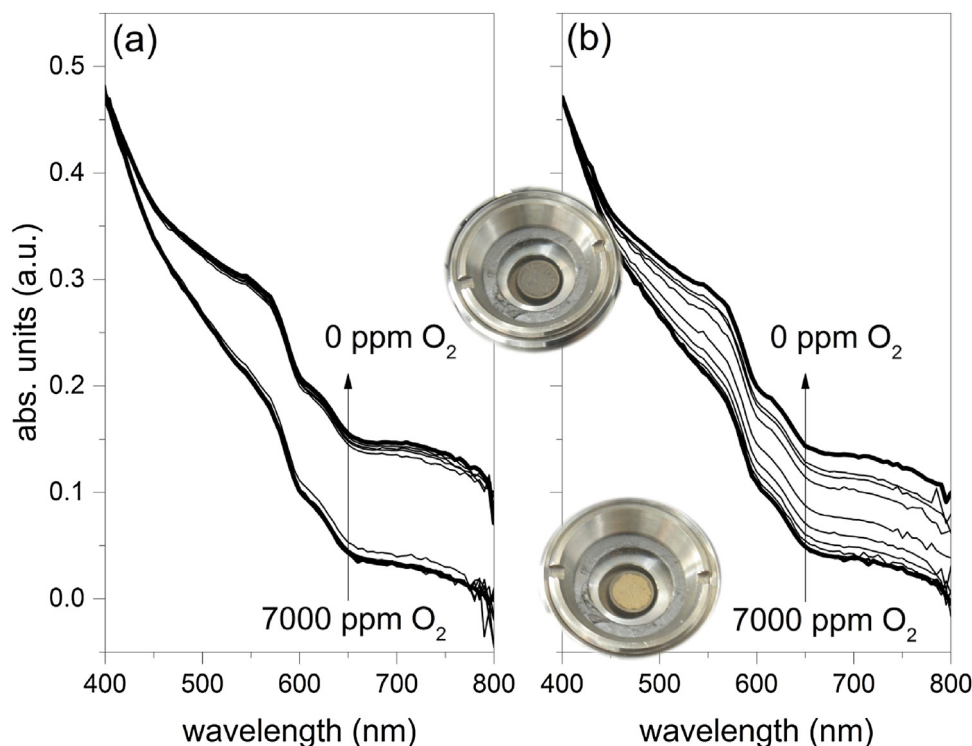


**Fig. 7.** Operando DRUV spectra obtained in continuous feed of 7000 ppm CO, 1500 ppm CH<sub>4</sub> and 5 vol% H<sub>2</sub>O while decreasing the O<sub>2</sub> concentration from 7000 ppm to nil (bottom to top) at 350 °C (a) in the absence and (b) in the presence of 1600 ppm NO. The two images on the bottom and on the top represent the sample in the spectroscopy cell under the feed containing 7000 ppm and 0 ppm O<sub>2</sub>, respectively. (For interpretation of the references to colour in this figure legend, the reader is referred to the web version of this article.)

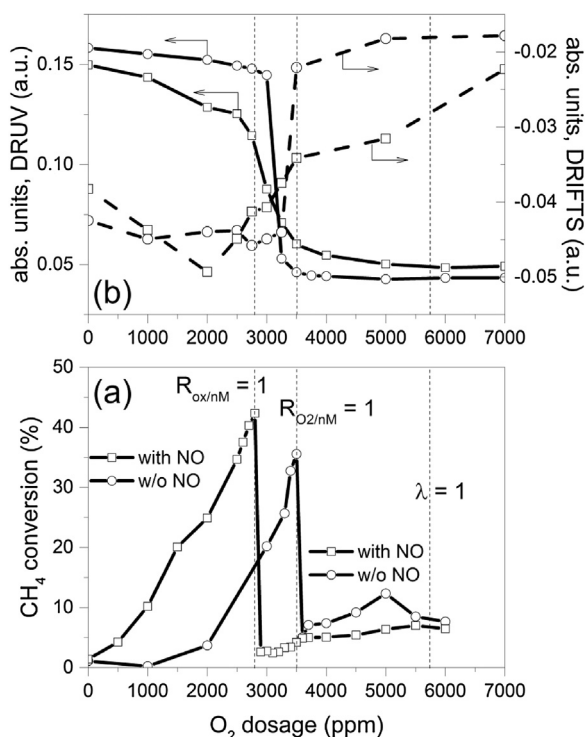


**Fig. 8.** (a) CH<sub>4</sub> conversion in continuous feed of 7000 ppm CO, 1500 ppm CH<sub>4</sub> and 5 vol% H<sub>2</sub>O at 350 °C while decreasing the O<sub>2</sub> concentration from 7000 ppm to nil (□) in the presence and (○) in the absence of 1600 ppm NO. (b) Evolution of the signal (solid line) at 650 nm in the DRUV data and (dash line) at 2501 cm<sup>-1</sup> in the DRIFTS data while decreasing the O<sub>2</sub> concentration from 7000 ppm to nil. The vertical dash lines mark the position of R<sub>ox/nM</sub> = 1, R<sub>O2/nM</sub> = 1 and λ = 1 (see text for details).

sequence of O<sub>2</sub> variation is shown in Fig. 8b. The baseline changed abruptly between 3500 and 3250 ppm O<sub>2</sub> in the absence of NO thus mirroring the change of oxidation state fingerprinted by the DRUV signal at 650 nm. Therefore, for analogy with the DRUV data we attribute these baseline changes to the change of oxidation state of Pd also in the case of the DRIFTS experiments [40]. Moreover, the smooth change of both signals at 2500 cm<sup>-1</sup> and at 650 nm can be correlated to the gradual consumption of nitrate species on the catalyst surface. Hence, in a catalytic system that apparently requires a significant portion of the PGM to be reduced because CH<sub>4</sub> abatement is most efficient under net reducing conditions, we may observe that nitrate species, e.g. more in general NO, maintain Pd oxidized [27]. This shifts the optimal point of CH<sub>4</sub> conversion to even richer conditions, where CH<sub>4</sub> oxidation by remaining O<sub>2</sub> and water becomes favored by the presence of reduced Pd.

We conclude by speculating on the situation the catalyst may experience under periodic rich/lean oscillations. The continuous change between rich and lean conditions on the one hand repeatedly changes the oxidation state of Pd between reduced and oxidized [41,42], the extent of oxidation and reduction depending plausibly on the extent of amplitude of O<sub>2</sub> concentration variation. On the other hand, it also guarantees that the conditions of oxidation state and speciation of the catalyst surface do not incur in one of the two extremes, either rich or lean conditions, over an extended period of time.

#### 4. Conclusions

A honeycomb Pd-only three-way catalyst was subjected to various experimental conditions under both static and periodic operation in order to study the chemistry at work responsible for CH<sub>4</sub> oxidation. Despite the possibility that the observed behavior

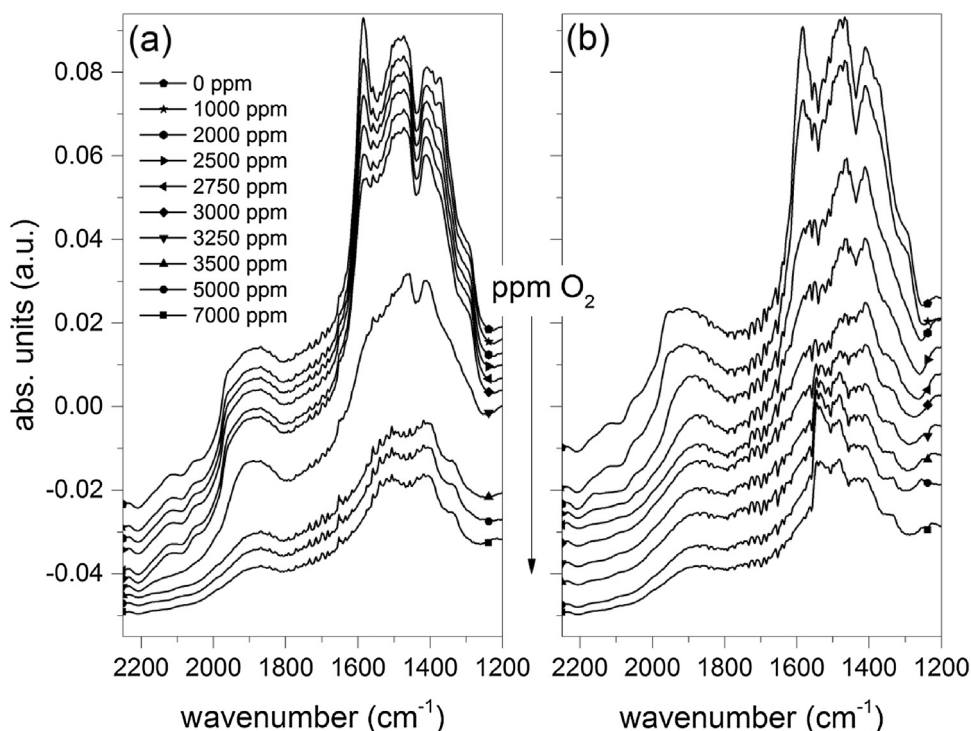


**Fig. 9.** Operando DRIFT spectra obtained in continuous feed of 7000 ppm CO, 1500 ppm CH<sub>4</sub> and 5 vol% H<sub>2</sub>O while decreasing the O<sub>2</sub> concentration from 7000 ppm to nil (top to bottom) at 350 °C (a) in the absence and (b) in the presence of 1600 ppm NO.

**Table 1**

Assignment of the vibrational modes of species observed in the DRIFT experiments of Fig. 9.

wavenumber (cm <sup>-1</sup> )	species	vibrational mode <sup>a</sup>	Ref.
1955 + 1909	Pd-CO	$\nu(\text{CO})$	[36]
1585 + 1376	bridged formates <sup>b</sup>	$\nu_{\text{as}}(\text{OCO})$ and $\nu_{\text{s}}(\text{OCO})$	[35]
1514, 1415 and 1340	various carbonate species	$\nu_{\text{as}}(\text{OCO})$ and $\nu_{\text{s}}(\text{OCO})$	[34]
1545 and 1482	various nitrate species	$\nu_{\text{as}}(\text{ONO})$ and $\nu_{\text{s}}(\text{ONO})$	[37–39]

<sup>a</sup>  $\nu$ , stretching;  $\nu_{\text{as}}$ , asymmetric stretching;  $\nu_{\text{s}}$ , symmetric stretching;  $\delta$ , deformation mode.

<sup>b</sup> Beside  $\nu_{\text{as}}(\text{OCO}) + \delta(\text{C-H})$  and  $\nu(\text{C-H})$  modes at 2907 and 2838 cm<sup>-1</sup>, respectively, not shown in Fig. 9.

may be unique to the selected catalyst sample, the following points appear clear:

- the TWC demonstrated significant CH<sub>4</sub> oxidation activity only under periodic rich/lean reaction conditions and NO conversion essentially followed that of CH<sub>4</sub>;
- the point of optimal CH<sub>4</sub> conversion did not correspond to the nominal stoichiometric point ( $\lambda = 1$ ) but was placed under net reducing conditions; this was clearly demonstrated by comparison with operation using propene as representative hydrocarbon of gasoline that satisfied the conventional stoichiometric point;
- CO inhibited CH<sub>4</sub> oxidation: this was demonstrated by the fact that the new stoichiometric point of optimal CH<sub>4</sub> conversion coincided with the complete removal of CO;
- CH<sub>4</sub> oxidation occurred likely via steam reforming under net reducing conditions;
- water inhibited CH<sub>4</sub> oxidation both under net reducing and net oxidizing conditions;
- NO was reduced most likely by the H<sub>2</sub> produced by steam reforming and water gas shift rather than by CO;
- NO shifted the point of optimal CH<sub>4</sub> conversion into net reducing conditions but also increased the overall CH<sub>4</sub> oxidation activity;
- NO inhibition under net oxidizing conditions was most likely induced by formation of nitrate species that were identified by operando infrared spectroscopy;
- under oscillating rich/lean reaction conditions, CH<sub>4</sub> oxidation was significantly enhanced and the amplitude of the oscillations appeared more crucial than their frequency;
- operando spectroscopy also identified the transition from oxidized Pd to metallic Pd when passing from net oxidizing to net reducing conditions, which coincided with the point of optimal CH<sub>4</sub> conversion; the transition was abrupt in the absence of NO while it was smooth in the presence of NO as a result of the persistence of oxidized Pd in the presence of NO.

The observation that the very same catalyst did not perform well in CH<sub>4</sub> oxidation under static conditions compared to periodic rich/lean conditions and that the amplitude of rich/lean oscillations significantly affected CH<sub>4</sub> oxidation activity hold important implications for the development of suitable catalysts and control strategies for optimal abatement of CH<sub>4</sub> from vehicles fueled with natural gas.

## Acknowledgments

A. Marberger is kindly acknowledged for support with the spectroscopic measurements. This work was conducted in the framework of the Swiss Competence Center for Energy Research (SCCER) BIOSWEET program.

## References

- [1] E.K. Nam, T.E. Jensen, T.J. Wallington, *Environ. Sci. Technol.* 38 (2004) 2005–2010.
- [2] A. Raj, *Johnson Matthey Technol. Rev.* 60 (2016) 228–235.
- [3] R.J. Farrauto, R.M. Heck, *Catal. Today* 51 (1999) 351–360.
- [4] T. Mailliet, C. Solleau, J. Barbier, D. Duprez, *Appl. Catal. B* 14 (1997) 85–95.
- [5] H.S. Gandhi, G.W. Graham, R.W. McCabe, *J. Catal.* 216 (2003) 433.
- [6] R.M. Heck, R.J. Farrauto, *Catalytic Air Pollution Control*, 3rd edition, John Wiley and Sons, Inc., Hoboken, New Jersey, 2009.
- [7] G. Beulertz, M. Votsmeier, R. Moos, *Appl. Catal. B* 165 (2015) 369–377.
- [8] S.H. Oh, P.J. Mitchell, *Appl. Catal. B* 5 (1994) 165.
- [9] P.J. van den Brink, C.M. McDonald, *Appl. Catal. B* 6 (1995) 197.
- [10] K.R.J. Subramanian, M.S. Chattha, *Ind. Eng. Chem. Rev.* 31 (1992) 2460.
- [11] P. Gelin, M. Primet, *Appl. Catal. B* 39 (2002) 1–37.
- [12] D. Ciuparu, M.R.L.E. Altman, L.D. Pfefferle, A. Datye, *Catal. Rev. Sci. Eng.* 44 (2002) 593–649.
- [13] T.V. Choudhary, S. Banarjee, V.R. Choudhary, *Appl. Catal. A* 234 (2002) 1–23.
- [14] P. Forzatti, G. Groppi, *Catal. Today* 54 (1999) 165–180.
- [15] M.F.M. Zwinkels, S.G. Järas, P.G. Menon, *Catal. Rev. Sci. Eng.* 35 (1993) 319–358.
- [16] R.J. Farrauto, M.C. Hobson, T. Kennelly, E.M. Waterman, *Appl. Catal. A* 81 (1992) 227–237.
- [17] T.R. Baldwin, R. Burch, *Appl. Catal.* 66 (1990) 337–358.
- [18] M. Salaün, A. Kouakou, S. Da Costa, P. Da Costa, *Appl. Catal. B* 88 (2009) 386–397.
- [19] D. Bounechada, G. Groppi, P. Forzatti, K. Kallinen, T. Kinnunen, *Appl. Catal. B* 119–120 (2012) 91–99.
- [20] H. Ohtsuka, *Emiss. Control Sci. Technol.* 1 (2015) 108–116.
- [21] M. Kleemann, M. Elsener, M. Koebel, A. Wokaun, *Appl. Catal. B* 27 (2000) 231–242.
- [22] C. Brinkmeier, *Automotive Three Way Exhaust Aftertreatment Under Transient Conditions: Measurements, Modeling and Simulation*, University of Stuttgart, Stuttgart, 2006.
- [23] M. Skoglundh, P. Thormählen, E. Fridell, F. Hajbolouri, E. Jobson, *Chem. Eng. Sci.* 54 (1999) 4559.
- [24] S.K. Matam, G.L. Chiarello, Y. Lu, A. Weidenkaff, D. Ferri, *Top. Catal.* 56 (2013) 239.
- [25] R.M. Heck, R.J. Farrauto, S.T. Gulati, *Catalytic Air Pollution Control: Commercial Technology*, John Wiley & Sons, Hoboken, New Jersey, 2009.
- [26] J.A. Botas, M.A. Gutierrez-Ortiz, M.P. Gonzalez-Marcos, J.A. Gonzalez-Marcos, J.R. Gonzalez-Velasco, *Appl. Catal. B* 32 (2001) 243–256.
- [27] V. Marchionni, M. Nachtegaal, A. Petrov, O. Kröcher, D. Ferri, *J. Phys.: Conf. Ser.* 712 (2016) 012051.
- [28] R. Gholami, M. Alyani, K.J. Smith, *Catalysts* 5 (2015) 561–594.
- [29] N. Sadokhina, G. Smedler, U. Nylen, M. Olofsson, L. Olsson, *Appl. Catal. B* 200 (2017) 351.
- [30] D. Bounechada, G. Groppi, P. Forzatti, K. Kallinen, T. Kinnunen, *Top. Catal.* 56 (2013) 372–377.
- [31] C. Langhammer, Z. Yuan, I. Zoric, B. Kasemo, *Nano Lett.* 6 (2006) 833–838.
- [32] G. Agostini, E. Groppo, A. Piovano, R. Pellegrini, G. Leofanti, C. Lamberti, *Langmuir* 26 (2010) 11204–11211.
- [33] G.R. Rao, H.R. Sahu, *Proc. Indian Acad. Sci. Chem. Sci.* 113 (2001) 651–658.
- [34] C. Morterra, G. Magnacca, *Catal. Today* 27 (1996) 497–532.
- [35] O. Pozdnyakova, D. Teschner, A. Wootsch, J. Kröhnert, B. Steinhauer, H. Sauer, L. Toth, F.C. Jentoft, A. Knop-Gericke, Z. Paal, R. Schlögl, *J. Catal.* 237 (2006) 1–16.
- [36] T. Lear, R. Marshall, J.A. Lopez-Sanchez, S.D. Jackson, T.M. Klapötke, M. Bäumer, G. Rupprechter, H.J. Freund, D. Lennon, *J. Chem. Phys.* 123 (2005) 174706.
- [37] I. Nova, L. Castoldi, L. Lietti, E. Tronconi, P. Forzatti, F. Prinetto, G. Ghiotti, *J. Catal.* 222 (2004) 377–388.
- [38] J. Baltrusaitis, J. Schuttlefield, J.H. Jensen, V.H. Grassian, *PCCP* 9 (2007) 4970–4980.
- [39] J. Szanyi, J.H. Kwak, R.J. Chimentao, C.H.F. Peden, *J. Phys. Chem. C* 111 (2007) 2661–2669.
- [40] T. Bürgi, R. Wirz, A. Baiker, *J. Phys. Chem. B* 107 (2003) 6774–6781.
- [41] A. Eyssler, E. Kleymentov, A. Kupferschmid, M. Nachtegaal, S.K. Matam, P. Hug, A. Weidenkaff, D. Ferri, *J. Phys. Chem. C* 115 (2011) 1231–1239.
- [42] J. Nilsson, P.A. Carlsson, S. Fouladvand, N.M. Martin, J. Gustafson, M.A. Newton, E. Lundgren, H. Grönbeck, M. Skoglundh, *ACS Catal.* 5 (2015) 2481–2489.